Biological Image Edge Extraction Based on Adaptive Beamlet Transform

Van Hau Nguyen*, Kyung-Haeng Woo**, Won-Ho Choi**

Abstract

In cell biology area, microscopy enables detecting objects inside cells that are stained or fluorescently tagged. It is disadvantageous for observing these objects because of the noisy characteristics of their environmental surrounding. In this paper, a framework is proposed to increase the throughput and reliability for analysis of these images. First, we apply adaptive beamlet transform to extract edges meaningfully followed by orientation, location, and length in different scales. Then, a post-process is implemented to extend and map them onto original image. Our proposed scheme is compared with Canny edge detector and conventional beamlet transform from four evaluation aspects. It produces better results when experiments are conducted on real images. Much better results for observing internal parts make this framework competitive for analysis of cell images

Keywords : Adaptive beamlet transform, cell boundary observation, evaluation criterions, edge extraction

I. Introduction

The analysis of biological images is a time consuming task in many microbiological and biomedical laboratories. There is an ever-increasing need for analyzing large numbers of images acquired with microscopes in connection with different assays, where one wishes to measure the number of cells, the size of certain objects, the area occupied by cells, etc [1]. Recent years a number of methods have been developed to facilitate some of these tasks [2-3][4]. Nevertheless, many of the tasks are still performed manually, and there is a great need for accurate and reliable methods that can automate the image analysis and thus increase the throughput in these assays.

Edge is one of the most important features in images, which contains lots of information. The effect of edge detection has a numerous influence on image segmentation and pattern recognition [5]. The problem of edge detection has a long history in computer vision. The simplest edge detection schemes compute the approximate gradient of the intensity map of the image by applying a filter, such as the Sobel, Prewitt or Roberts filter [6], and then use a thresholding to extract the edges identified as areas with large gradient. other methods use the second derivatives of images and search for zero-crossings instead of maxima. More sophisticated edge detectors such as the one developed uses the intensity gradient, after it has been appropriately smoothed, search for local maxima only in the gradient direction, and apply additionally a hysteretic thresholding to maximize the edge connectivity. However, they are still difficult to extract features embedded in extremely high noise or the SNR (signal to noise) is so low that none of the pixel values is likely to yield significance. Biological images such as available from electron or light microscopy are rather sensitive to noise and when smoothing is applied to reduce the noise, the edges also are smoothed to the extent that they cannot be detected.

A number of edge detection methods employ 2D Gabor filters. These filters are characterized by frequency, width and direction and have been mainly applied to object recognition problems [7]. Other powerful edge detection methods are also available, such as snakes or active contours , which also use gradient information from the image to evolve a connected contour that minimizes its energy in the landscape defined by the image [8][9]. These methods successfully detect boundaries of objects with an intensity difference compared to the background, but in biological images, it is often the case that the interior and the exterior of the object of interest show no difference in intensity.

* Vietnam National University ** Ulsan University

투고 일자 : 2010. 11. 9 수정완료일자 : 2011. 4. 8
게재확정일자 : 2011. 4. 30

* This work was supported by the 2008 Research Fund of University of Ulsan.

In this paper, we design a framework to extract the edge in the biological images, with challenge characteristics mentioned above, based on adaptive beamlet transform. Beamlets can be generated by recursive dyadic partitioning, vertex marking and connecting. The beamlet transform [10] is the collection of all line integrals formed by viewing the image as a piecewise constant object and integrating along line segment in the beamlet dictionary, and draw a line segment depicting that beamlet. All these beamlets in different scales are fused to generate an edge map at the image pixel level. The proposed method detects lines with any orientation, location and length in different scales and a maximal beamlet coefficient is computed to avoid subjective setting. The output results after extending and mapping edges show better performance than conventional methods with evaluation criterions as well as with detecting for real images. It can be suitable to apply this scheme to detect objects for biological image processing.

In the next section, background about the characteristics of biological images and beamlet transform approach are shown. The framework and implementation of edge detection are presented in section III. The experiment and results are given in section IV, and section V brings to the conclusions.

II. Background

A. Biological Image Characteristics

Biological specimen images are often low-contrasted. Although negative staining with heavy metal is used, the contrast is still not sufficient to separate clearly the membranes from the background with a simple threshold method. The stain tends to outline the structure of the specimen, but the gray level of the membrane itself is still very low, unless it is coated with stain or aggregated. The more interesting areas, the crystal-like non-aggregated membranes to be studied at high magnification, are the more difficult to identify [11]. Then, among the drawbacks of staining, artifacts and uneven staining are those that can complicate the segmentation at the medium magnification. This leads to a heterogeneous gray level of the background and an uneven contrast and width of the edges [12]. Finally, the size and the shape of the objects can vary greatly. Thus, the identification of the membranes based on pattern approach could not appropriate.

B. Beamlet Transform

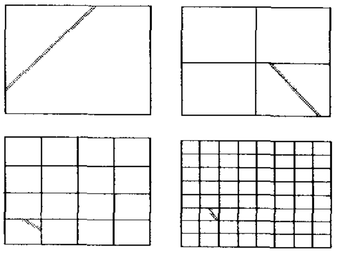

Fig. 1. Four Beamlets at various scales, locations, and orientations.

We consider an image as a function residing on a $[0,1]\times[0,1]$ unit square. It is a piecewise constant, with pixels of side 1/n by 1/n. The collection of beamlets $B_{n,\delta}$ is a multi-scale collection of line segments occurring at a full range of orientations, positions, and scales. It is generated as following [10].

Dyadic Subdivision: We form all dyadic sub-squares of $[0,1]^2$ in the obvious way; to begin we divide the unit into four sub-squares of side length 1/2. Each sub-square is then divided into four smaller sub-squares, and so on. Fig. 1 shows some sub-squares after 0, 1, 2 or 3 steps of subdivision. We continue until we have created all dyadic squares of side 1/n-by-1/n or larger.

Vertex Labeling: For definiteness, think of σ as 1/n, although in certain applications σ should be far smaller. Traversing the boundary of each sub-square, we mark out equally spaced vertices at spacing. Note that the distance between neighboring vertices is σ, no matter which scale sub-square we consider.

Connection of the dots: In each sub-square, form the collections of all line segments connecting any pair of vertices. Any such line segment is called a beamlet.

Let $f(x_1,x_2)$ be a continuous function on $[0,1]^2$. The beamlet transform of f is the collection of all line integrals.

$$T_f(b) = \int_b f[x(l)]dl, b\in B_{n,\delta} \qquad (1)$$

The integrals are being taken along line segments $b\in B_{n,\delta}$. Here $x(l)$ traces out the beamlet b along a unit speed path. The digital beamlet transform of an $n\times n$ array (f_{i_1,i_2}) is understood to be the beamlet transform of the function f which is defined on the continuum by interpolation of the values (f_{i_1,i_2}).

$$f(x_1,x_2) = \sum_{i_1,i_2} f_{i_1,i_2}\phi_{i_1,i_2}(x_1,x_2) \qquad (2)$$

Where $\phi_{i_1,i_2}(x_1,x_2)$ is a specified family of continuous interpolation functions. There are several ways the functions $\phi_{i_1,i_2}(x_1,x_2)$ may be chosen. The functions $\phi_{i_1,i_2}(x_1,x_2)$ may be chosen to obey the conditions

$$n^2 \int_{pixel(i'_1,i'_2)} \phi_{i_1,i_2}(x_1,x_2) dx_1 dx_2 = \delta_{i_1,i'_1} \cdot \delta_{i_2,i'_2} \tag{3}$$

Where $\delta_{i,i'}$ is the Kronecker symbol. Then f is a function that obeys

$$f_{i_1,i_2} = Ave\{f | pixel(i_1,i_2)\} \tag{4}$$

In other words, the values of f_{i_1,i_2} are viewed as pixel-level averages of the continuous function f.

C. Extraction of features

Suppose we have a noisy $n \times n$ image, perhaps contains somewhere within it, a faint image of a line segment of unknown length, orientation and position [13-14]. We model these data as following

$$y_{i_1,i_2} = A \bullet \overline{\phi_{i_1,i_2}} + \varepsilon z_{i_1,i_2} \quad 0 < i_1,i_2 < n \tag{5}$$

Where ε is a noise level z_{i_1,i_2} is a white Gaussian noise. A is an unknown parameter and $\overline{\phi_{i_1,i_2}} = \tilde{\phi}(i_1,i_2,\nu_0,\nu_1)$ is the observed effect at the sensor array of an unknown beamlet $\overline{\nu_0,\nu_1}$. The problem is to set the simple null hypothesis

$$H_0 : A = 0 \tag{6}$$

against the composite alternative

$$H_1 : A > 0 \quad \nu_0,\nu_1 \in [0,1]^2 \tag{7}$$

where H_0 denotes for square decorated by choosing scale level, and H_1 denotes for square left undecorated.

This is composite because of the wide range of possible endpoint pairs being considered. We consider the random field

$$Y[\nu_0,\nu_1] = \langle \Psi_{\overline{\nu_0,\nu_1}}, y \rangle = \max\{T_y(b) / \sqrt{L(b)}\} \tag{8}$$

Where $T(y)$ is the beamlet transform of data y. $L(b)$ is the Euclidean distance of beamlet b. $\Psi_{\overline{\nu_0,\nu_1}}$ is the filter matched to $H_{1,\overline{\nu_0\nu_1}}$.

$$\Psi_{\overline{\nu_0\nu_1}}(i_1,i_2) = \frac{\tilde{\phi}(i_1,i_2,\overline{\nu_0\nu_1})}{\| \tilde{\phi}(i_1,i_2,\overline{\nu_0\nu_1}) \|} \tag{9}$$

We reject H_0 if $Y[0,1]$ exceeds a certain threshold. Fig.2 shows the extraction of feature in an image.

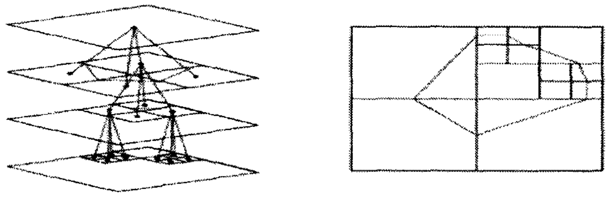

Fig. 2. A beamlet decorated recursive dyadic partition and its associated structure.

D. Beamlet Transform of each square

After we obtain each square from the image, we take the transformation onto each sub_square as detailed below.

Step 1: Start from northwest corner point in the sub-square, vertices are marked clockwise at equal distance as $p(0), p(1), p(2), \ldots, p(pnum-1)$. Where $pnum$ is the number of points on the boundary of sub-square.

Step 2: Set start-point $p(0)$, end-point $p(l)$, a start-point and an end-point correspond to a line segment b .

Step 3: Locate all pixel points in the line segment through interpolation methods introduced above. Pixel points are $l(0), l(1), \ldots, l(lnum-1)$ where $lnum$ is the number of pixels point in the line segment.

Step 4: Calculate sum of grey value of all pixel point in one line segment

$$sum = \sum_{i=0}^{lnum-1} G(d(i)) \tag{10}$$

where $G(d)$ denotes the gray value of pixel at point d.

Step 5: Calculate beamlet transform of the line segment

$$T_f(b) = \sum sum / lnum \tag{11}$$

```
Step 6: Check the below conditions:
If start-point is not $p(num-1)$,
 {end-point=end-point+1;
  repeat step 3, step 4, step 5    }
 else
 {star-point=start-point+1;
   if start-point=$p(num)$, {procedure stop}
    else {repeat step 3, step 4, step 5}   }
```

III. The Proposed Method

A. Algorithm of Edge Extraction

As mentioned above, it encounters much challenge for methods to extract the edge in the biological images in applications, especially low-light ones such as fluorescence microscopy. Here, we proposed a novel method to handle kinds of these images, based on adaptive beamlet transform.

The algorithm of [10] is proposed to extract line from the images. There are two problems when using this algorithm to detect edge directly. Discrete beamlet transform algorithm firstly needs set a certain threshold and test the simple null hypothesis to decide whether to draw a line segment to depict one beamlet. The problems can arise if the threshold is low and much noise in the image, and erroneous edge lines might be generated. To overcome this, we calculate a maximal beamlet coefficient to avoid subjective setting and declare pixels as edge pixels if gradient magnitude is larger than those of pixels at its both sides in the direction of maximum intensity change as stated in [15][16]. The second problem is that the formula $T(b)/\sqrt{L(b)}$ defined in eq.(8) needs to be searched for the maximum, otherwise for the minimum when the gray value of line is larger than surrounding one. Yet, on the edge of the gray images, the gray value could be larger or smaller than surrounding one. Therefore, we improved the algorithm of [10], and proposed a new edge detection algorithm for gray images. A new parameter is defined as $BC_s = T(b)/L(b)$, which represents the weighted average of gray value in current beamlet. In every dyadic square, the parameters of the beamlet that may be the most probable edge in every direction are compared, then the edge is determined eventually.

The algorithm for the proposed method is described as following steps:

Step 1: Set the scale of image squares of $nWidth \times nHeight, s = s_0$.

Step 2: Decompose the image into scale fixed sub-squares according to recursive dyadic partitioning, each sub-square is $\frac{nWidth}{2^{s_0}} \times \frac{nHeight}{2^{s_0}}$

Step 3: Transform each sub-square.

Step 4: The parameter of every beamlet is calculated in current direction $BC_s = T(b)/L(b)$. *T(b)* is the beamlet transform of image along *b*, and *L(b)* is the Euclidean length of a beamlet.

Step 5: In current direction, all of the beamlets are analyzed one by one. Suppose the parameter of current beamlet is BC_{s1} ,the parameters of two beamlets adjacent are BC_{s2} and BC_{s3}, BC_r is calculated

$$BC_r = |BC_{s1} - BC_{s2}| + |BC_{s1} - BC_{s3}| \qquad (12)$$

where BC_r is the beamlet coefficient at the current direction.

Step 6: The maximum of beamlet coefficient ($Max - BC_r$) following the current direction is calculated in current direction . If $Max - BC_r$ is larger than BC_r , BC_r will be updated with the new value. The starting point and the terminal point of the beamlet corresponding to $Max - BC_r$ are preserved.

Step 7: The maximum of $Max - BC_r$ is calculated in all dyadic squares of an image. We define the maximum of $Max - BC_r$ of all dyadic squares as M and make the normalization

$$Max - BC_r = Max - BC_r / M \qquad (13)$$

Step 8: Using specified threshold *Th*, with $0 < Th \le 1$, then mark selected pixels with gradient magnitude larger than *Th* as strong pixels, and weak pixels corresponding to pixels with magnitude less than *Th*.

Step 9: Select all strong pixels, and all weak pixels that are connected to strong pixels in all directions.

Step 10: Extend the extracted edges along the directional field computed to connect neighboring edge segments.

Step 11: Map the edges onto the original image and perform processing suitable to the application.

B. Extending the Edges along the Directional Field

Even though the thresholding in algorithm is designed to reduce 'streaking' (the subdivision of edges into short segments), the edges that are extracted from steps 1 to step 9 of algorithm are not always connected to the desired extent. The reason for this may be that the influence of nearby edges prevents some pixels from being local maxima, so that they are ruled out by the non-maximal suppression, or some pixels have a value smaller than the low threshold. However, they are actually parts of the edge.

As a remedy, the edges may be extended as follows: starting at the end points of the already selected edge segments, we take a step in the direction given by the directional field, away from the edge segment we start at. We then continue moving along the directional field until a specified number of steps have been taken, or we end up on a different edge segment. If we end up on a different edge segment, the entire path we moved along is included as an edge. A threshold is also employed to exclude pixels with small magnitude to be included in the extension.

C. Post Processing

The output from the scheme described so far is not always, what one would like to present as a final output. In particular, one might want to make sure that the edges form a connected loop, remove isolated edge segments, and thin the edges. Furthermore, since parameters are not defined on the same grid as the original image, the selected edges will need to be interpolated onto the original image grid. This post-processing has to be adapted to the particular application.

IV. Experiment and Results

A. Evaluation Criterions

In order to analyze the performance of the proposed algorithm quantification, we have applied an evaluation method as in [17]. By comparison with Canny algorithm, our method is evaluated from fours aspect: continuity of the edge, rate of wrong detection, rate of miss detection, and anti-noise performance.

Line-fit degree L of edge: For every detected edge pixel (i,j), we compute the number $n_{i,j}$ of other edge pixels in its 3×3 neighboring window. If $n_{i,j}<2$, the edge pixel (i,j) is judged as an isolated point, otherwise a joint point. We define

$$L=1-\frac{Num_{iso}}{Num_{total}} \tag{14}$$

where Num_{iso} is the number of isolated points, Num_{total} is the number of edge pixels. As we know, the larger the Num_{iso}, the smaller the line-fit degree is.

Detection degree of false edges R_e: Num_{false} denotes for the number of pixels on the edge detected. Those pixels also belong to the smooth area of referenced edge image. Num_{total} denotes for the number of pixels that belong to the smooth are in referenced image. The rate of wrong detection is given as

$$R_e=\frac{Num_{false}}{Num_{total}} \tag{15}$$

Non-detection degree of true edges R_l: Num_{omit} presents the number of undetected pixels of true edge compared with reference image. The rate of miss detection is defined as

$$R_l=\frac{Num_{omit}}{Num_{total}} \tag{16}$$

Parameter E is a total evaluation, which is the weighted sum of three parameters defined below

$$E=\alpha L+\beta(1-R_e)+\gamma(1-R_l) \tag{17}$$

where $\alpha+\beta+\gamma=1$. α, β, and γ are the weighted coefficients. The more parameter E is close to one, the better the performance of scheme is.

B. Results and Discussion

We will implement the testing 256×256 gray image to inform and sketch out the very high adaptation for biological images. The evaluation method needs a reference edge image to compare with others. Here, the reference image is as in Fig.3(b). The Canny algorithm, method using beamlet transform and our proposed method are used to detect edge respectively. In Canny algorithm, we choose the parameters: 0.05 and 0.25. In our method, we implement at scale 6, threshold *Th=0.2*. The weighted coefficients to evaluate are chosen as $\alpha=0.3,\beta=0.4,\gamma=0.3$.

When there is no noise, the result images of Canny algorithm and beamlet transform algorithm are shown as Fig.3(c) and Fig.3(d) respectively. Our result is shown in Fig.3(e) and Fig.3(f). After that, we change the noise by adding noise at different levels. The edge of Canny method, by using beamlet, by using only adaptive beamlet and, by using our scheme is shown as Table 1

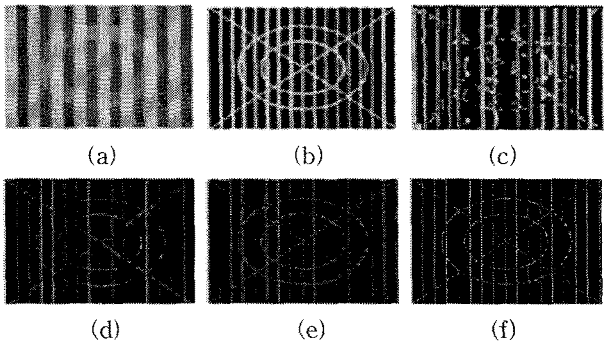

Fig. 3. Testing image to evaluate the performance of each method (a) Test image (b) Reference edge image (c) Edge detected by using Canny's method (d) Edge detected by using beamlet transform (e) Edge detected by using adaptive beamlet (EAB) (f) Edge by extending and mapping (EEM).

In the image of Fig.3(a), there are two oblique lines, the output of Cany algorithm is inferior while beamlet transform method and our algorithm perform much surpassing results. The proposed algorithm of detecting the edge from gray images is of better continuity. The rate of wrong detection and miss detection are lower than beamlet transform method. The anti-noise performance of edge extraction by using only adaptive beamlet transform is a little lower than beamlet method. However, it is very important to compare the total evaluation parameter by using complete framework. The post-processing step helps it robust to noise influence. As illustrated in Fig.4, this parameter E of our scheme is always better than one of beamlet method. It is evident that the proposed algorithm can adapt to the very noisy images and work with the surpass performance. They are essential factors to apply this method for processing biological images that are low-contrast, much noisy.

Table 1. Parameters of performance

SNR	Algorithm	L	$1-R_e$	$1-R_l$	E
no noise	Canny	0.832	0.831	0.826	0.830
	Beamlet	0.978	0.997	0.983	0.987
	EAB	0.980	0.999	0.994	0.992
	EEM	**0.982**	**0.999**	**0.994**	**0.992**
100db	Canny	0.830	0.826	0.824	0.827
	Beamlet	0.978	0.997	0.983	0.987
	EAB	0.980	0.999	0.988	0.990
	EEM	**0.980**	**0.999**	**0.994**	**0.992**
70db	Canny	0.828	0.826	0.820	0.825
	Beamlet	0.978	0.997	0.983	0.987
	EAP	0.975	0.998	0.987	0.988
	EEM	**0.978**	**0.998**	**0.988**	**0.989**
50db	Canny	0.824	0.824	0.817	0.822
	Beamlet	0.978	0.977	0.983	0.979
	EAB	0.975	0.996	0.985	0.986
	EEM	**0.978**	**0.996**	**0.985**	**0.987**
20db	Canny	0.821	0.820	0.813	0.818
	Beamlet	0.964	0.992	0.974	0.978
	EAB	0.970	0.992	0.980	0.982
	EEM	**0.972**	**0.993**	**0.980**	**0.982**

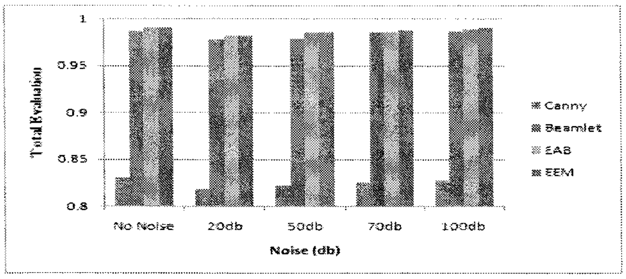

Fig. 4. The total evaluation of each method with different noise.

We apply our method to an electron microscopy image showing a vesicle with some internal structure as in Fig.5(a). Our intention is to find the outer membranes of the vesicle.

This task is difficult for several reasons. The image is noisy and full of small structures, so it will detect edges everywhere. Furthermore, smoothing the image will not help much, since it will smooth the thin edges as much as the other structures, making it harder to detect the edges. It is important to note that edge linking is one of vital task cell boundary extraction [18]. An edge is the boundary between an object and the background, and indicates the boundary between overlapping objects. This means that if the edges in an image can be identified accurately, all of the objects can be located and basic properties such as area, perimeter, and shape can be measured. This requires a plain of edges detected [4].

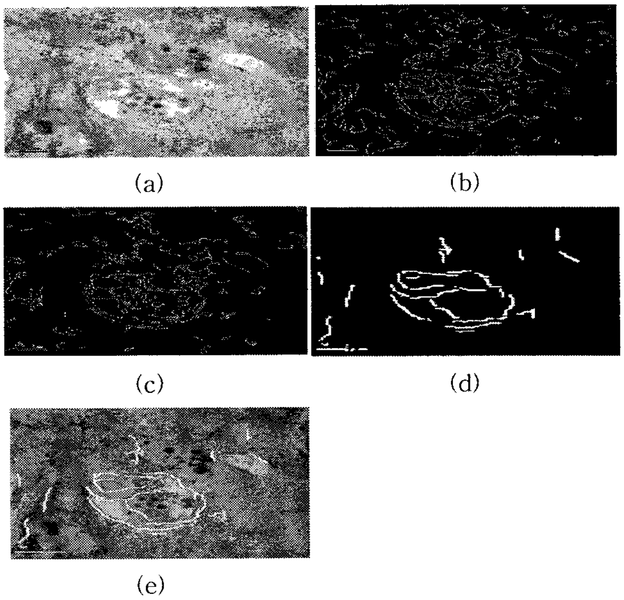

Fig. 5. Edge extraction on a microscopy image of a vesicle (a) Original image: an electron microscopy image of a vesicle (b) Edge extraction using Canny (c) Edge extraction using beamlet transform (d) Edge extraction using our proposed method (e) The final results of the edge extraction overlaid on the original image, after the edges have been extracted and extended along the directional field to connect the different edge segments.

Beamlet provide a multi-scale decomposition of the image that makes it possible to pick just a few scales and ignore for example of the finest scale, where most of the noise is, and the coarsest scale, where the large differences in intensity are. Beamlet also provide us with information about directionality in the image, which enables us to search for structures with a strong direction, and trace along them.

The final result using threshold 0.33, and extending the edges along the directional field to connect the adjacent edge segments, is shown on Fig. 5(e), with the edges overlaid in white on the original image. The outer membranes of the vesicle are successfully detected almost everywhere, and the most prominent internal membranes are also detected by our proposed scheme.

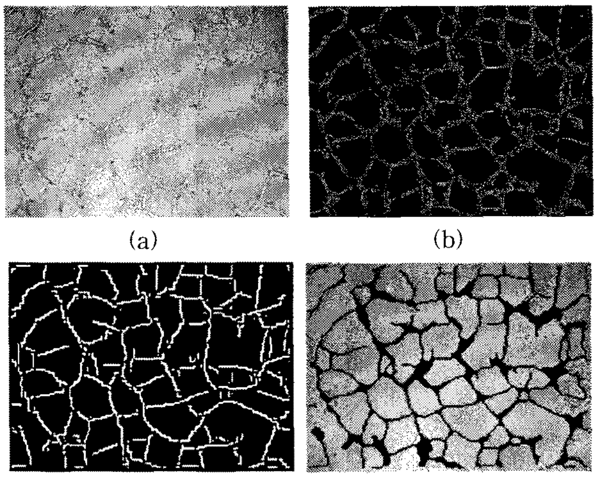

Fig. 6. Edge detection on the tube formation assay (a) Original image: an image of a tube formation assay (b) Edge extraction using beamlet transform (c) Edge extraction using our proposed method (d) The output result of the edge extraction overlaid on the original image.

Our edge detection scheme is compared to the method using conventional beamlet transform. The thresholds have been chosen to show the edges of the vesicle clearly, while eliminating the surrounding structures as much as possible. It is clear that our scheme detects the vesicle membranes better than the other. The conventional beamlet and Canny gives multiple responses to the membranes as shown in Fig.5(b) and Fig.5(c), and detects most of the smaller structures, which makes it hard to distinguish the interesting structures from the background.

As a second example, our method was applied to a light microscopy image from a tube formation assay as in Fig. 6(a). In a tube formation assay, endothelial cells are grown on a dish, and their ability to form vessels (or tubes) is investigated by counting the number of tubes seen in the image and computing their length, as well as extracting network information such as the number of junctions. This example is used to show how elongated multicellular structures can be detected using our scheme. In the Fig. 6(c), the results from the edge detection scheme are overlaid in black on the original image. The edges have been extended to connect adjacent edges. Finally, the edges were dilated and then thinned to fill possible holes in the selected areas. Almost all of the tubes are detected, only a few weaker tubes are not marked. The broader, sheet-like structures are marked because they show internal intensity variations, and in some cases two parallel tubes have been joined together because they can not be distinguished at the level we use.

From above experiments, our proposed scheme performs a little superior than other methods using evaluation criterion stated in [17]. However, it is noted that we implement these results to only validate for ability to apply this scheme for biological image processing. In other words, as experimental results of real images, although other methods extracted edges exactly, it is hard to determine the boundary of cell correctly due to many detected edges as in Fig.5(b-c) and Fig.6(b). A post-processing step to extend and map edges in our framework can overcome these problems by outputting plain edges as illustrated in Fig.5(d) and Fig.6(c).

V. Conclusions

In this paper, a framework was proposed to extract the edge with various orientation, location and length based on adaptive beamlet transform. Here, the beamlet transform was adapted to detect and track edges in very noisy images. The experiment results showed preponderant performance in comparison with Canny edge detection and conventional beamlet transform about four aspects: continuity of edges, wrong detection, miss detection rate, anti-noise performance. On the other hand, by figuring out a post-processing step, the method become more powerful to process the biological images which can overcome many limitations in vision.

References

[1] Meijering E, van Cappellen G, "Quantitative biological image analysis," in *Imaging cellular and molecular biological functions*, Edited by: Shorte SL, Frischknecht F. Berlin: Springer Verlag, pp. 45-70, 2007.

[2] Murashov, D.M. "A Two-level Method for Segmenting Cytological Images Based on Active Contour Model," *Pattern Recognition and Image Analysis*, Volume 18, pp. 177 - 192, 2008.

[3] Yang Qihua, Wang Qiang, "Tissue Cell Boundaries Detection based on Curvelet-based Snake Model in Electrorotation Bio-chip Control System," *BioMedical Engineering and Informatics, BMEI 2008*, vol.1, pp. 728-732, 2008.

[4] Changming Sun, Pascal Vallotton, Dadong Wang, Jamie Lopez, Yvonne Ng, David James, "Membrane boundary extraction using circular multiple paths," *Pattern Recognition in Computational Life Sciences*, Volume 42, Issue 4, pp. 523-530, 2009.

[5] Hui Zhang, Jason E. Fritts, Sally A. Goldman, "Image segmentation evaluation: A survey of unsupervised methods," *Computer Vision and Image Understanding*, Volume 110, Issue 2, pp. 260-280, May 2008.

[6] Parker, James R, *Algorithms for Image Processing and Computer Vision*, New York, John Wiley & Sons, Inc., pp. 23-29, 1997.

[7] Mehrotra R, Namuduri KR, Ranganathan N, "Gabor filter-based edge detection," *Pattern Recogn*, 25(12 pp. 1479-1494, 1992.

[8] Kass M, Witkin A, Terzopolous D, "Snakes- active contour models," *Int J Comput Vision*, 1(4) pp. 321-331, 1987.

[9] Candès EJ, Donoho DL, "New tight frames of curvelets and optimal representations of objects with piecewise C-2 singularities," *Commun Pur Appl Math.*, 57(2) pp. :219-266, 2004.

[10] Donoho D L, "Beamlet pyramids: A new form of multi-resolution analysis, suited for extracting lines, curves, and objects from very noisy image data," in *Proceeding of SPIE*, volume 4119, July 2000.

[11] A. Karathanou, J.-L. Buessler, H. Kihl and J.-P. Urban R, "Background Extraction in Electron Microscope Images of Artificial Membranes,"in *IFIP Advances in Information and Communication Technology*, Volume 296/2009, pp. 165-173, 2009.

[12] Campilho, Aurélio, Coudray, Nicolas, Buessler, Jean-Luc, Kihl Hubert, Urban, Jean-Philippe, "Multi-scale and First Derivative Analysis for Edge Detection in TEM Images," *Image Analysis and Recognition*, Lecture Notes in Computer Science, Springer 2007, pp. 1005-1016, 2007.

[13] A. Averbuch, R.R. Coifman, D.L. Donoho, M. Israeli, and J. Walden, "Fast slant stack: A notion of radon transform for data on a Cartesian grid which is rapidly computable, algebraically exact, geometrically faithful, and invertible," *Tech. Rep.*, Stanford University, 2001.

[14] D. L. Donoho and X. Huo, "Beamlets and multiscale image analysis," in *Proc. Multiscale and Multiresolution Methods*, vol. 20, pp. 149-196, Lecture Notes in Computational Science and Engineering, 2002.

[15] Canny J, "A computational approach to edge-detection," *IEEE T Pattern Anal.*, 8(6) pp. 679-698, 1986.

[16] R. Deriche, "Using Canny's Criteria to Derive a Recursively Implemented Optimal Edge Detector," *Int'l J. Computer Vision*, pp. 167- 187, 1987.

[17] Xuan Yang and Dequn Liang, "A New Edge Evaluation Using Region Homogeneous Measure," *Journal of Image and Graphics*, vol. 4, no. 3, pp. 234-238, Mar. 1999.

[18] Ling, Wing-Kuen and Tam, Kwong-Shun, "Closed boundary extraction of cancer cells using fuzzy edge linking technique," *In SPIE Symposium-Image Processing: Algorithms and Systems*, San Jose, 2002.

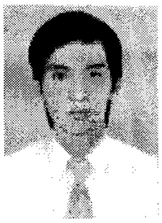

Van Hau Nguyen received the B.S. degree in electronic physics from Vietnam National University - Hochiminh City, University of Natural Sciences in 2006.

He is currently working towards M.S degree on electrical engineering.

His research interests include the areas of image processing and digital signal processing.

Kyung Haeng Woo received the B.S., M.S. degree in electronic engineering from University of Ulsan in 1993 and 1995, respectively. From 1998 to 2000 she worked at Samchang co. Ltd., as a R&D member.

From 2005 to 2010 she worked at E&I tech as a president. From 2010 until the present she has been with the University of Ulsan, and now she is a guest professor at the School of Electrical Engineering.

Her research interests include the image processing and computer vision.

Won Ho Choi received the B.S., M.S., and Ph.D. degree in electronic engineering from Yonsei University in 1978, 1980, and 1990, respectively.

From 1980 to 1985 he worked at Jeil Precision and Hewlett-Packard as a R&D member.

From 1986 until the present he has been with the University of Ulsan, and now he is a professor at the School of Electrical Engineering.

His research interests include the image processing algorithm/hardware design.